



CST0008

Modification and validation of a rigid hybrid III 50th male dummy model under crash test

Burawich Muangto*, Pattaramon Jongpradist

Department of Mechanical Engineering, Faculty of Engineering, King Mongkut's University of Technology Thonburi, 126 Pracha-uthit Rd., Bangmod, Thungkru, Bangkok 10140, Thailand

* Corresponding Author: burawichmuangto@gmail.com, +668-9691-0190

Abstract. In the evaluation of occupant injury severity through finite element analysis, a Hybrid III 50th percentile male dummy is usually used to assess the risk of injury under crash test. The aim of this paper is to study and amend the rigid finite element dummy model to effectively capture the actual kinematics and more precise injury data during the crash. Modifications have been made to the modeling of the waist, shoulder, femur and ankle joints of the rigid dummy model based on the properties of the physical dummy. The modified dummy model is validated through simulation of dynamic sled testing under the initial velocity of 56 km/h (30 mph). The injury parameters from the original rigid dummy model from Hypercrash and those of the modified dummy model including the acceleration of the head, the acceleration of the thorax and the upper neck moment are then measured and compared with the existing experimental data. Finite element results for different initial velocities are also investigated. The proposed model is proved to be able to satisfactorily improve the prediction fidelity of the dummy mechanism and severity of the occupant's injury under frontal collisions.

1. Introduction

Road traffic accidents are globally one of the leading causes of death [1]. Studies of occupant responses and injury mechanism during crashes are necessary to develop vehicle design able to reduce the severity of accidents. In the automotive industry, the full scale anthropomorphic are often used in crash tests to investigate the behaviors of human bodies and record data concerning the evaluation of injury criteria. Although the full scale anthropomorphic in crash test is ideal, the tests are rather complicated with the high cost for instrumentation and required expertise. As a result, finite element modeling is a preferable alternative approach to investigate response of real human in road accidents. In frontal crash testing, the occupant dummies representing the average adult males universally employed to assess the injury risk is the Hybrid III 50th percentile male dummy [2, 3]. The data necessary in the assessment of injury characteristics due to frontal impact consist of head acceleration, thorax acceleration, upper neck force, upper neck moment and the femur force [4, 5]. Therefore, it is necessary to validate and ensure that the measures from finite element simulation can appropriately represent the actual incident.

Sled tests are conducted to represent a simple frontal collision by applying initial velocity and deceleration to the occupant dummy. The tests are primarily used to confirm the performance of occupant restraint system and validate the dummy effect between physical test and finite element simulation. Kent et al. [6] used Madymo rear-seat occupant sled test model to verify the injury of Hybrid III 50th percentile male dummy and 5th percentile female dummy with different seat-belt parameters and

impact speed. It was found that head strikes and chest acceleration in a female dummy were generally lower than those in a male dummy. Mohan et al. [7] used LS-DYNA to validate the Hybrid III family developed with Livermore Software Technology Corporation (LSTC) and National Crash Analysis Center to ensure the accuracy, efficiency and robustness. The finite element results were found to be reasonably correlated to the test results. Human finite element models have also been improved to accurately apprehend local injury mechanisms. Kennerly et al. [8] developed Hybrid III 50th percentile male dummy with leg bone model to estimate ankle injuries under offset crash. The leg bone model indicated smaller rotation in dorsiflexion and larger rotations in inversion and eversion which effect to ankle injuries. Iwamoto et al. [9] improved the head/face, shoulder and internal organ of THUMS finite element model and validated the results with cadaver tests. The proposed model was tested and shown to be comparable with multiple real world accident situations by accident reconstruction considering rib fracture and skull fracture.

Although detailed dummy models with fully deformable parts, such as Madymo, LSTC and THUMS models, are shown to impressively demonstrate the actual behavior of occupant during crashes. The models typically contain an extremely large number of nodes that require a considerable CPU run time. For non-contact crashes, a rigid body dummy model can be an adequate representation to examine the occupant kinematics and injury risk. The run time for rigid body models are significantly less than the deformable dummies and, in that sense, is more efficient. This research aims to study the implementation of a rigid body dummy from Hypercrash to dynamic sled test and develop a modified partly-deformable dummy model able to represent the occupant mechanism and injury risk during frontal crash while maintaining the simplicity of the simulation model and its analysis.

2. Computational Model

Sled systems provide repeatable and reliable impact conditions around which automotive seats, seat belts, and supplemental restraints can be developed [10]. Sled tests are common in the comparison and validation of the dummy responses between experimental set-up and finite element results in which the dynamic conditions of a full-scale crash in accidents are allowed. The initial and imposed velocity profile are applied to sled systems in order to characterize the vehicle velocity before and during crash accidents.

The finite element model in this study consists of a dummy model and a sled system as shown in Figure 1. The dummy model is a rigid body Hybrid III 50th percentile male imported from Hypercrash with the total weight of 78 kg. The body of the dummy is meshed with 5,004 4-noded shell elements and 25 spring elements are located at all required measurement sensors. The seat structure consists of 6,500 8-noded brick element of seat cushion, 17,318 4-noded shell elements of seat frame and floor, and 7 beam elements of seat belt. The seat frame is made of steel and the seat cushion is visco-elastic polyurethane close-cell foam with density of 100 kg/m³ and Young's modulus of 15 MPa. The seat belt is made of fabric with an assigned pretensioner stroke of 50 mm width and 6,000-N load-limiter. Fatal injuries from frontal collision can occur at the occupant's head, neck and thorax. Thus, in the current study, the injury measurement points model are detected at those positions illustrated in Figure 1.

Two dummy models are used in the analysis, i.e., the original rigid body dummy and a modified rigid body dummy with deformable joints. In the latter model, rigid body condition is assigned to all parts except for the shoulder joints, waist joint, femur joints and ankle joints as shown in Figure 2. So as to allow realistic dynamic movement of the dummies during crashes. The mechanical properties of the deformable parts are based on those applied to LSTC model [11].

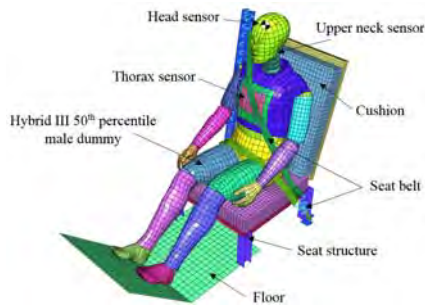


Figure 1. FE model of sled system and a rigid body occupant dummy

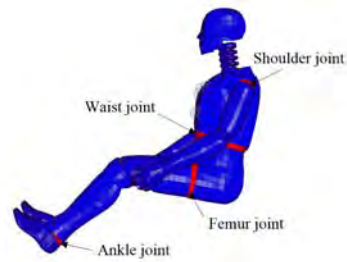


Figure 2. Modification of rigid dummy model with deformable joints

The dummies are placed on the seat cushion in a regular sitting position by using multi-usage surface-to-surface contact. The cushion and the seat frame contacts are tied to each other. A node-to-surface contact is assigned to the dummy feet and the floor. Interface penetrations between all contact surfaces are eliminated by shifting the slave nodes in seat cushion from the master surfaces of the dummy model. The initial velocity of 56km/h in x-direction is assigned to all nodes in the model as displayed in Figure 3. The function of an imposed velocity profile as shown in Figure 4 is assigned only to the seat frame and the floor to simulate vehicle's deceleration during frontal collision. From the time instants 10 ms to 30 ms, the velocity is decreased representing braking of the vehicle with deceleration of 5.8g. Then, the velocity is abruptly reduced from collision with acceleration pulse of 29.6g during the time instants of 30 ms to 80 ms until the car stops.

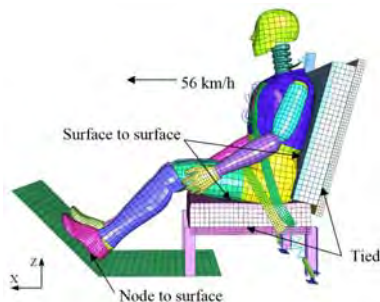


Figure 3. Boundary conditions and initial velocity applied to the sled test model

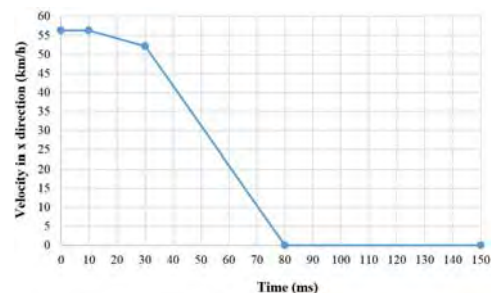


Figure 4. Imposed velocity function applied to model

3. Results and Discussions

Sled tests simulations are performed by dynamic explicit finite element analysis using RADIOSS solver. The head resultant velocity, thorax resultant velocity and pelvis resultant velocity of the rigid body dummy model and the modified model are illustrated in Figure 5(a) to (c), respectively. The solid lines represent results of rigid body dummy model while the dashed lines show results of the modified dummy model. The triangular markers display the prescribed velocity of the vehicle.

The time histories of resultant velocities from the two models show similar trend. The resultant velocities decrease corresponding to the imposed velocity of the sled system especially at the pelvis location where the dummy is restrained by the seat belt. The resultant velocities at the head and thorax of the rigid body model also strictly follow the imposed velocity profile and approach zero when the sled stops at the time instant reaches 80 ms. This is due to mobility limitations of the rigid body dummy model. After the sled stops, the resultant velocities of all parts slightly increase due to rebound effect. In contrast, since the modified dummy model possesses more moveable joints, the inertia effect causes the thorax and head movements last 10 ms and 40 ms longer than those of the original model before the rebound occurs.

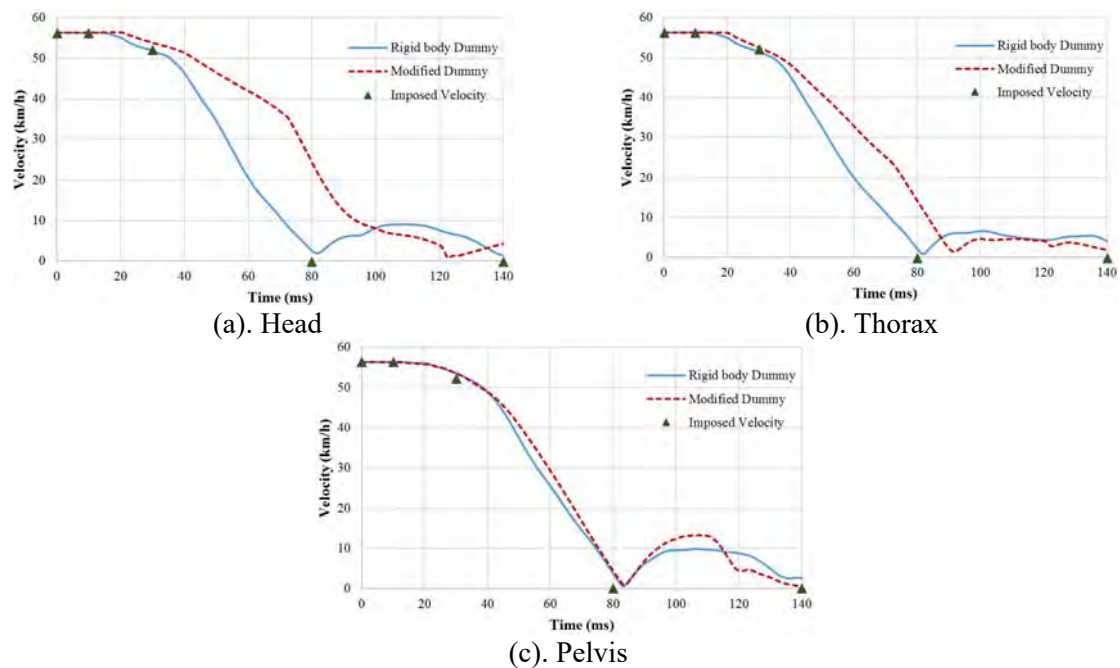


Figure 5. The resultant velocities at different parts of dummy models

The dummy's movement behaviors of the rigid body dummy model and the modified dummy model are compared with the sled test experiment by Mohan et al. [7] as shown in Figure 6. The dummy kinematics of the rigid body dummy are different from experimental results whereas the modified dummy is able to precisely capture the dummy mechanism. There are two factors that affect the dummy's motions. First, the upper torso and pelvis parts are rigidly attached by the seat belt and therefore can only have limited movement. This prevents the upper torso to bend. Second, since the shoulder joints, femur joints and ankle joints are rigid, arms and feet are prevented from swinging up. In the modified dummy model, the aforementioned joints are changed to deformable parts. Therefore, during the vehicle braking, the upper torso can bend down. Arms and feet can swing up and the head can move forward. This results in the analogous dummy's movements between the modified dummy model and the experiment.

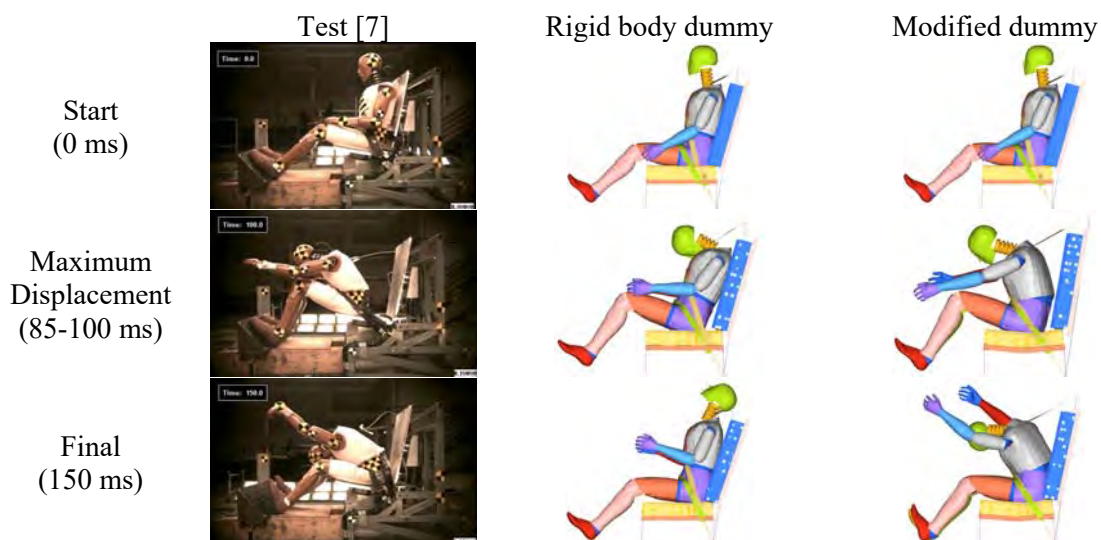


Figure 6. Dummy movement at different time instances

Head trajectories in x and z-axis during the sled test are shown in Figure 7(a). In the rigid dummy model (shown by the solid blue line), the dummy's head moves forward and down to the maximum of $x = 112$ mm and $z = -171$ mm at time instant of 88 ms. Then, the dummy's head swings back to the starting position where $x = 0$ mm at the time 240 ms. The head trajectory of the modified dummy model (shown as a dashed red line) moves much farther forward to the maximum displacement of $x = 395$ mm and $z = -367$ mm. In this case, the head returns to the starting position at the instant 400 ms which is much slower than the results obtained from the rigid dummy model. Similar behaviors are observed for the thorax displacements. The thorax of the rigid dummy model moves in a limited space between the position where $x = 17$ mm, $z = -27$ mm at 81 ms and $x = 19$ mm, $z = 13$ mm at 178 ms while the maximum thorax displacement in the modified dummy model is the forward position of $x = 176$ mm and $z = -69$ mm and back to the position of $x = 35$ mm and $z = -11$ mm at 357 ms. In addition, Figure 7 shows that assigning deformable joints to the modified dummy model leads to increase in forward movements of the dummy and lower the head and thorax swing-back displacements compared to the rigid body model.

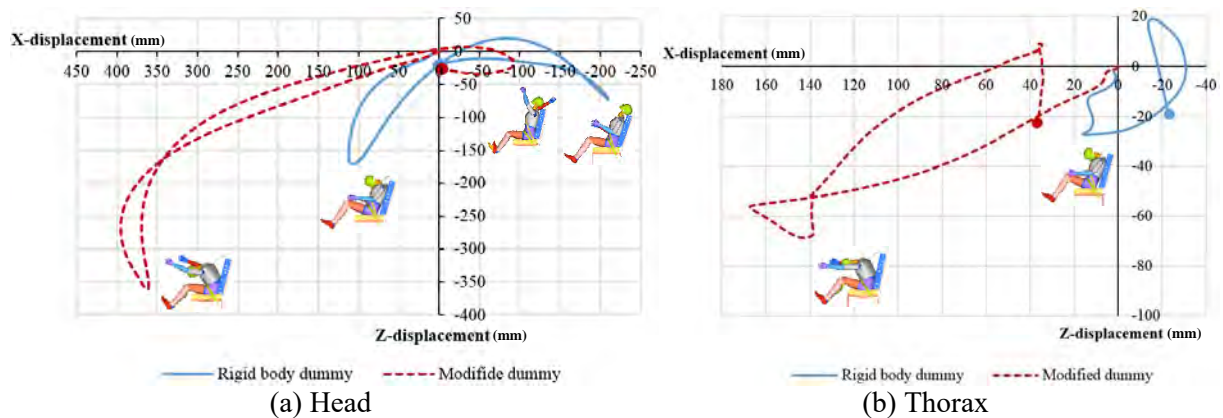


Figure 7. The trajectories at different parts of dummy

The comparisons between the head resultant acceleration, the upper neck moment, and the thorax resultant acceleration of the rigid body dummy model, the modified dummy model, and the experimental test performed on physical dummy are shown in Figures 8-10, respectively. It can be clearly seen that the time history measurements from the modified dummy match the experimental result considerably better than those from the rigid body dummy. Moreover, the maximum values of the rigid body dummy model occur earlier than other cases because of the kinematic behaviors of dummy. Figure 8 shows that the maximum head accelerations of all cases are about 55g-60g, which occurs at 60 ms for rigid body model and 80-90 ms for the modified dummy and the actual test. Figure 9 plots the upper neck moment used in neck injury criteria calculation. The maximum upper neck moment of the rigid body model is 130 N.m, which occurs at about 80 ms. The maximum upper neck moment of the modified body model and physical model are 80 N.m and 38 N.m, respectively. The upper neck moment in the rigid body model is higher due to rigidity of the thorax at time instant 125 ms. Therefore, the dummy's neck absorbs all the inertia forces from impact. The maximum thorax accelerations of all cases are about 38g-43g. However, the modified model has a second peak equal to 45g caused by chin movement contacting the thorax. This contact does not occur to the physical dummy in the experiment because the dummy leans farther forward. Further adjustment to the modified dummy should be performed to correct this result.

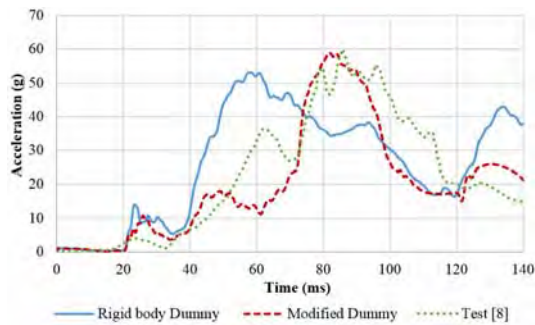


Figure 8. Head resultant acceleration

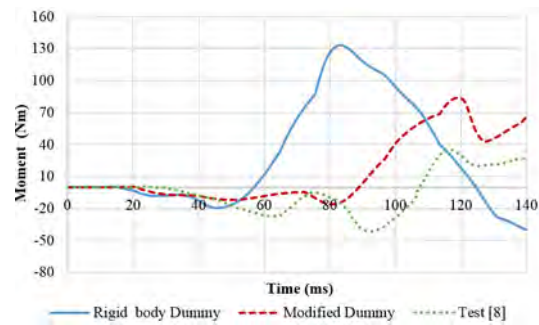


Figure 9. Upper neck moment

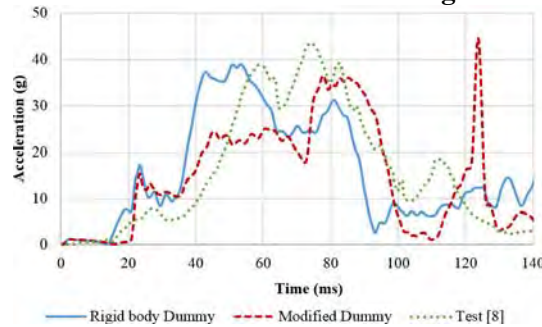


Figure 10. Thorax resultant acceleration

Next, the initial velocity is varied to investigate the trend of injury parameters presented in Figure 8-10. Three initial velocities of 30 km/h, 56 km/h (baseline) and 70 km/h, are applied to the sled model. The maximum values of the injury parameters and the time instants when the maxima occur are listed in Table 1. It is noticed that the peaks of head resultant acceleration, upper neck moment, and thorax resultant acceleration for all initial velocities occur at about the same time whereas their magnitudes correspond to the applied velocities. Although the movement behavior of the rigid dummy model can not represent the correct kinematics of the real test, the head and thorax resultant accelerations are comparable with results from the modified dummy model. Nonetheless, the upper neck moments are greatly overestimated and cannot be used in injury criteria considerations when the rigid body model is employed.

Table 1. Results of injury parameters for different initial velocities

Initial Velocity (km/h)	Maximum Head resultant acceleration (g)		Maximum Upper neck moment (N.m)		Maximum thorax resultant acceleration (g)	
	Rigid body	Modified	Rigid body	Modified	Rigid body	Modified
30	25 (57ms)	23 (86ms)	87 (90ms)	71(120ms)	23 (54ms)	19 (58ms)
56 ^a	53 (58ms)	59 (82ms)	133(83ms)	80 (119ms)	39 (53ms)	37 (78ms)
70	66 (59ms)	68 (80ms)	158 (79ms)	102 (115ms)	46 (46ms)	41 (69ms)

^a Baseline velocity

4. Conclusion

This paper presents application and modification of the finite element model of a rigid Hybrid III 50th percentile male dummy from Hypercrash to effectively evaluate the occupant kinematics and injury severity during dynamic sled test. Due to the lack of mobility in the original model, the rigid dummy does not show good correlation to the movement behaviour of the physical dummy. Alteration of the model by applying deformable shoulder, waist, femur and ankle joints can substantially improve the fidelity of the rigid dummy. The occupant mechanism under frontal crash as well as the related injury parameters including the acceleration of the head and thorax and the upper neck moment are shown to match with the data from experiment.

References

- [1] Road traffic injury; <http://www.searo.who.int/thailand/areas/gsr-thai.pdf?ua=1>, accessed on 02/08/2017.
- [2] Zhao G, Xie L and Guo Y, 2009, *Analysis and Evaluation on the Rear-end Crash of the Car with a Dummy*, International Conference on Measuring Technology and Mechatronics Automation , P.475-478.
- [3] Muangto B, Jongpradist P, 2016, *Study on Effectiveness of Frontal Crash Standards for Passenger Bus using Finite Element Analysis*, The 7th TSME International Conference on Mechanical Engineering, Thailand .
- [4] Luo X, Du W and Zhang, 2015, *Safety Benefits of Belt Pretensioning in Conjunction with Precrash Braking in a Frontal Crash*, Intelligent Vehicles Symposium, June 28–July 1, Korea.
- [5] Linder A, Schick S, Hell W, Svensson M, Carlsson A, Lemmen P, Schmitt K and Gutsche A, Tonasch E, 2013, *ADSEAT-Adaptive seat to reduce neck injuries for femal and meal occupant*, Accident Analysis & Prevention, p.334-343.
- [6] Kent R, Forman J and Parent D, Kuppa S, 2007, *Rear seat occupant protection in frontal crashes and its feasibility*, Proceedings of the 20th Conference on the Enhanced Safety of Vehicles, June 18-21, 2007, Layon, France, p.1-13.
- [7] Mohan P, Park C, Marzougi D, Kan C, Guha S, Maurath C and Bhalsod D, 2010 *LSTC/NCAC Dummy Model Development*, 11th international LS-DYNA user conference, Detroit, USA.
- [8] Digges K and Bedewi P, 1997, *HYBRID MODELLING OF CRASH DUMMIES FOR NUMERICAL SIMULATION*, IRCOBI Conference, Hannover, Germany.
- [9] Iwamoto M, Kisanuki Y, Watanabe I, Furusu K and Miki K, 2002, *DEVELOPMENT OF A FINITE ELEMENT MODEL OF THE TOTAL HUMAN MODEL FOR SAFETY (THUMS) AND APPLICATION TO INJURY RECONSTRUCTION*, IRCOBI Conference, Munich, Germany, September 18-20.
- [10] Sled Test Development; https://www.exponent.com/experience/sled-test-development/?_page_size=NaN&_page_num=0&loadAllByPage_size=true, accessed on 14/06/2017.
- [11] LSTC Dummy Models for LS-DYNA; http://www.lstc.com/download/dummy_and_barrier_models, accessed on 12/01/2017.